The Day the Sun Stood Still: Using global Thermodynamic MHD Simulations to Infer the Structure of the Solar Corona and Inner Heliosphere during the Maunder Minimum

Pete Riley, Roberto Lionello, and Jon A. Linker

Predictive Science, 9990 Mesa Rim Road, Suite 170, San Diego, CA 92121, USA.

pete@predsci.com and lionel@predsci.com

Leif Svalgaard

Stanford University, HEPL, Via Ortega, Stanford, CA 94305 USA

leif@leif.org

Ed Cliver

AFRL/RVBXS, Sunspot, CO 88349 USA

ecliver@nso.edu

Andre Balogh

Imperial College, South Kensington Campus, Department of Physics, Huxley Building 6M68, London, SW7 2AZ, UK

a.balogh@ic.ac.uk

Jürg Beer

Surface Waters, Eawag, Ueberlandstrasse 133, P.O. Box 611, 8600 Duebendorf, Switzerland

Juerg.beer@eawag.ch

Paul Charbonneau

Département de Physique, Universit de Montral, C.P. 6128 Centre-Ville, Montral, Qc, H3C-3J7, Canada

paulchar@astro.umontreal.ca

Nancy Crooker and George Siscoe

Center for Space Physics, Boston University,725 Commonwealth Avenue, Boston, MA 02215, USA

crooker@bu.edu and siscoe@bu.edu

Marc DeRosa

Lockheed Martin Solar and Astrophysics Laboratory, 3251 Hanover St., B/252, Palo Alto, CA 94304, USA

derosa@lmsal.com

Mike Lockwood

University of Reading, Department of Meteorology, Earley Gate, P.O. Box 243, Reading, Berkshire, RG6 6BB, UK

lockwood@reading.ac.uk

Ken McCracken

100 Mt. Jellore Lane, Woodlands, NSW, 2575, Australia

jellore@hinet.au

Matt Owens

Department of Meteorology, University of Reading, Reading RG6 6BB, UK

m.j.owens@reading.ac.uk

Ilya Usoskin

Sodankyla Geophysical Observatory, FIN-90014, University of Oulu, Finland

ilya.usoskin@oulu.fi

Yi-Ming Wang

Naval Research Laboratory, 4555 Overlook Ave SW, Washington DC 20375-5252, USA

yi.wang@nrl.navy.mil

and

S. Koutchmy

Institut d'Astrophysique de Paris, CNRS and UPMC, Paris, France

koutchmy@iap.fr

Received _____; accepted _____

To be submitted to Ap. J.

ABSTRACT

Observations of the Sun's corona during the space era have led to a picture of relatively constant, but modulating solar output and structure. Longer-term, more indirect measurements, such as from ^{10}Be, coupled by other albeit less reliable contemporaneous reports, however, suggest periods of significant departure from this standard, which may possibly have produced terrestrial weather effects. The Maunder Minimum, was one such epoch where: (1) Sunspots effectively disappeared for long intervals during a 70-year period; (2) Eclipse 'observations' suggested the distinct lack of a visible K-corona but possible appearance of the F-corona; (3) Reports of aurora were notably reduced; and (4) Cosmic ray intensities at Earth were inferred to be substantially higher. Using a global thermodynamic MHD model, we have constructed a range of possible coronal configurations for the Maunder Minimum period and compared their predictions with these limited observational constraints. We conclude that the most likely state of the corona during the Maunder Minimum was not merely that of the 2008/2009 solar minimum, as has been suggested in several recent studies. Instead, we argue that the Sun's photospheric magnetic field was substantially reduced (by up to an order of magnitude) and this resulted in, and is consistent with the observations associated with this period.

Subject headings: Solar Corona; Solar Wind; MHD Simulations

1. Introduction

The "Maunder Minimum" is a period of time between approximately 1645 and 1715 when the observed number of sunspots all but disappeared (Eddy 1976). Although it can be argued how accurate the sunspot record was during this interval, the low numbers cannot be due to a lack of observations; a number of well-known astronomers, including Giovanni Domenico Cassini, regularly made observations of the Sun during this time. During the same period of time, as we will discuss in more detail below, the number of aurora decreased, cosmic ray fluxes increased, and the Sun's corona apparently lost its visible structure. Perhaps even more intriguingly, this period coincided with the so-called "Little Ice Age," during which time both North America and Europe experienced bitterly cold winters (e.g., Luterbacher (2001)).

Broadly speaking, we can differentiate between two distinct ideas for the state of the solar corona during the Maunder Minimum. The first, and original idea was of a corona that was radically different from what we observe today (Eddy 1976; Parker 1976; Suess 1979). The second, and currently more favored interpretation is of a corona that was not significantly different than the one observed during the recent and somewhat unique solar minimum of 2008/2009 (Svalgaard & Cliver 2007; Schrijver et al. 2011; Wang & Sheeley 2013).

In his landmark paper, (Eddy 1976) reviewed an extensive range of available data associated with this time period, including auroral records, sunspots, carbon-14 records, and eclipse observations. From the (i) prolonged absence of sunspots; (ii) reduction in aurora reports; (iii) decrease in ^{14}C (suggesting a significant increase in cosmic ray flux hitting the Earth); and (iv) absence of any structured corona during eclipses, he inferred that, to manifest such phenomena, the solar corona must have existed in a unique configuration. He suggested that "the solar wind would have blown steadily and isotropically, and possibly

at gale force, since high-speed streams of solar wind are associated with the absence of closed structure in the solar corona." He had concluded that, based on eclipse observations, there likely was not any K-corona present, and that, in fact, what was observed could have been from dust-scattered light (i.e., the F-corona). When asked about the Maunder minimum, Parker (1976) suggested "In view of the absence of a white light corona, we may conjecture whether the Sun was entirely shrouded in a coronal hole, yielding a fast steady solar wind, or whether there simply was no solar wind at all. I would guess the former, but I know of no way to prove the answer." Suess (1979) expanded on these views: "Firstly, C-14 data indicate an enhanced cosmic ray intensity, with the conclusion that the interplanetary magnetic field was smooth and perhaps of low intensity. Secondly, the apparent absence of a corona during eclipses requires low coronal density, suggesting an absence of closed magnetic loops. Thirdly, the absence of sunspots eliminates the possibility of a solar maximum type of corona of low emission intensity and implies a low large-scale photospheric field intensity. Finally, the absence of mid-latitude aurorae implies either that the solar wind speed or the IMF intensity, or both, were low and not irregular."

More recently, the idea that the Maunder Minimum was radically different than anything witnessed during the space era has come to be replaced with the idea that the recent, and undoubtedly unique solar minimum of 2008/2009 provided an accurate proxy for Maunder Minimum conditions. This perspective has been built up on two primary fronts. First, Svalgaard & Cliver (2007) proposed that there appears to be minimum value that can exist in the strength of the interplanetary magnetic field. It is important to recognize, however, that this is a hypothesis, not a robust empirically-determined result. Although the strength of the IMF has apparently returned to the same approximate value since the start of the space era, there is no guarantee that this must remain so, in fact, the precise value of this "floor" had to be lowered as we witnessed the minimum of 2008/2009. Second, Schrijver et al. (2011) argued that there exists a minimum state of solar magnetic activity,

associated with the presence of small-scale ephemeral regions. They concluded that "the best estimate of magnetic activity...for the least-active Maunder Minimum phases appears to be provided by direct measurements in 2008-2009." In perhaps what could be described as a compromise between these two extreme views, Wang & Sheeley (2013) presented a solution where the photospheric field consisted of ephemeral regions with a reduced, but not absent global dipole. They reasoned that a Sun consisting exclusively of ephemeral regions would generate no IMF, in conflict with the apparent continuation of the solar cycle (albeit much reduced) during the Maunder Minimum (McCracken et al. 2011).

Although our analysis focuses principally on inferring the likely structure of the corona and inner heliosphere during the Maunder minimum period, we are obliged to note that this period roughly coincided with an interval known as the "little ice age," during which time, the temperature in northern Europe was lower than normal, and sufficiently so that the river Thames froze over (Manley 2011). The connection, if any, between the two events, remains a topic of lively debate. Our main contribution to the discussion would be that if, on one hand, we conclude that the Sun during the Maunder minimum period was essentially the same as the 2008/2009 Sun, then it is very unlikely that there can be a causal connection between the Maunder minimum and the little ice age. On the other hand, if the Sun was radially different, then it at least opens the door for a variety of possible mechanisms to connect solar variability with Earth climate.

In this study, we apply a global MHD model to infer the most likely configuration of the solar corona (and by extension, the inner heliosphere) that is consistent with the observations associated with the Maunder Minimum. In section 2, we review, re-analyze, and extend previous studies of the limited, and often indirect observations of the period between 1645 and 1715. Our purpose is not to argue for a particular interpretation, but to identify and assess possible interpretations and estimate their uncertainties, even

qualitatively. In Section 3, we introduce a set of possible configurations of the photospheric magnetic field that may have existed during the Maunder minimum, and use them to drive MHD simulations. In Section 4, we describe our MHD formalism, paying particular attention to the unique aspects that make it applicable and relevant for studying the Maunder Minimum. In Section 4.4, we describe the model results and relate them to the 'observations,' allowing us to refute some configurations, whilst finding support for others. In Section 4.5, we develop a simple Bayesian, or conditional argument to assess the two principal hypotheses, which, while not definitively supporting or refuting either, does provide a heuristic way to weigh the various pieces of evidence. Finally, in Section 5 we summarize the main points of this study, and discuss the implications in terms of both understanding the Maunder Minimum and other periods of inactivity, the likelihood of future grand minima, and the possible correlation between such intervals and terrestrial climate.

2. "Observations" during the Maunder Minimum

Although a number studies since J. Eddy's landmark paper (Eddy 1976) have revised, and refined our interpretation of the available but limited "observations" associated with the Maunder minimum, it is worth reviewing them here, both to point out where they led to definitive inferences and where they remain ambiguous. Additionally, it affords us an opportunity to offer our own interpretation.

The "observations" we consider here are: (1) the sunspot time series; (2) aurora reports; (3) cosmic ray fluxes as inferred from 10-Be and 14-C records; and (4) eclipse observations. Figure 1 summarizes the first three of these records stretching back from near-present day to the Maunder minimum. In the following subsections, we consider each in more detail.

2.1. Sunspot "Observations"

Figure 1(a) summarizes the sunspot record back in time to 1610 (Svalgaard 2011). This is the parameter that originally defined the Maunder minimum, although the numbers themselves have undergone significant revision since they were first analyzed by G. Spörer and E. W. Maunder in the 1890's (Sporer 1887; Maunder 1894). As a practical definition, we follow the consensus of identifying the Maunder minimum as the time period between ~ 1645 and $\sim 1700-1715$ when sunspots all but disappeared. It is important to emphasize, however, that they did not disappear entirely; there were isolated observations of sunspots throughout this period. On the other hand, there were intervals of up to 25 years with virtually no sunspots being reported (Soon & Yaskell 2003).

The sunspot record is not without error or uncertainty, however. First, we must confront the claim that the reduction in sunspot number was not due processes at the Sun, but from a lack of observations. Hoyt & Schatten (1996) examined how well sunspots were observed during the Maunder Minimum, concluding, perhaps somewhat conservatively, that $68\% \pm 7\%$ of the days were observed. Therefore, the paucity of sunspots was due to them not being observed, not from there being no observations. Second, the apparent lack of sunspots may have been caused by atmospheric effects, such as the presence of volcanic ash masking the sunspots or increasing the threshold for detection. Third, the sunspot record has undergone revision over the years. Thus, the curve shown in Figure 1(a) differs from that of, say, Usoskin (2008) because of a renormalization of the last half century's worth of data. If such recent measurements have been found to be inaccurate, what does this suggest for records originating more than 300 years earlier? Although this could have a quantitative effect on the record, it is unlikely to change the basic, qualitative profile shown in Figure 1(a).

Assuming that the SSN record is a reliable proxy for the number of sunspots, we infer

that in ≈ 1645 they suddenly 'turned off,' and remained so until ≈ 1715. Thus, from the perspective of the SSN, the Maunder interval was a period of constant inactivity. It is worth noting here that the point in the solar cycle at which the Maunder Minimum began could have important theoretical ramifications. Mackay (2003) argued that if the Maunder Minimum began at solar maximum, this would have led to a configuration with effectively no unipolar polar fields. In contrast, if it began near, or at solar minimum, strong unipolar polar fields would have been present that may have remained intact to a large extent throughout the interval. On this question, Figure 1(a) is at best ambiguous.

At the risk of over-interpreting the signal, the SSN record during the Maunder Minimum further suggests that sunspots did cluster into perhaps half-a-dozen or so small peaks that may be suggestive of a continued solar cycle within the Maunder Minimum. Additionally, these cluster peaks, and the underlying base, tended to decrease slightly, perhaps suggesting that the Sun sank to even lower states of inactivity during the 70-year period. Finally, we note that the Maunder Minimum period terminated suddenly, or rather that solar activity resumed quite suddenly after 1700.

2.2. Aurora "Observations"

Records of aurora date back thousands of years (Siscoe 1980). Yet, again, interpreting them is fraught with danger. Does the absence of an aurora mean that one didn't occur, or just that it was not reported? Additionally, different records provide, at best, only threshold indicators of geomagnetic activity. Consistent observations at mid-latitudes, for example, will not contain modest geomagnetic events that reveal themselves only at the highest geomagnetic latitudes. Perhaps the strongest statement we can make is that if an aurora was observed, then it probably happened (there not being any other obvious phenomena that could mimic this effect), whereas, if none were reported, it may or may not

mean that none occurred. Thus, the auroral record, at least older than a century, at best, provides a lower limit of geomagnetic activity.

In spite of these limitations, several records exist and have been analyzed in detail. Here, for illustration, we rely on the dataset reconstructed by Réthly & Berkes (1963), however, our conclusions would not be affected had we used another set of measurements (e.g., Schröder (1992)). We consider the raw counts and smoothed profile shown in Figure 1(b) to make the following points. First, geomagnetic activity did not cease during the Maunder Minimum period. Second, activity was higher both before and after the Maunder minimum. Third, there is a tentative suggestion of a solar cycle modulation in the number of aurora days.

The presence of any aurora indicates that the Sun, through the solar wind, was connected to the Earth's upper atmosphere. To generate aurora requires a dawn-dusk electric field, which in turn, requires a roughly radially-directed solar wind carrying a B_z magnetic field. Additionally, at least some of the electrons and ions bombarding the atmospheric oxygen and nitrogen atoms presumably come directly from the solar wind. We conclude then, that Parker's suggestion that there might not be any solar wind at all, is not consistent with these observations.

Since these observations were made at mid-European latitudes, we can also infer that they were probably related to relatively substantial geomagnetic storms. This, in turn suggests that they originated not from corotating interaction regions (CIRs), which would tend to produce minor events, but from coronal mass ejections (CMEs). Further, we could anticipate that these CMEs were associated with the appearance of the relatively few sunspots that were present, signaling the presence of active regions. It is from active regions that the strongest (i.e., fastest and largest field strengths) are typically produced. Unfortunately, the limited number of auroral sightings during the Maunder minimum (one

at most in any one year, except once when two were observed) does not allow us to make a meaningful correlation between sunspot number and number of aurora. In contrast, later in the record, there is a significantly clearer correlation between the temporal location of the peaks in the two time series (although no obvious association in their amplitude).

In the context of modern times, how geomagnetically quiet was the Maunder Minimum? Unfortunately, these data had ceased to be recored by 1962. At most, during most of the Maunder Minimum period, only one aurora was observed at mid-latitudes in a single year, but during most years, no aurora were reported. In fact, during the 70 year period, only 5-6 events we reported. This once in more than a decade frequency is considerably lower than the time period from 1900-1963, when the Réthly & Berkes (1963) records stopped. Unfortunately, aurora are not generally counted in modern times. Therefore, we again conclude that these aurora data likely represent a lower limit for geomagnetic activity.

As a final point, as noted earlier, to penetrate to mid-latitudes, the solar source must be relatively significant. Thus, it is unlikely that corotating interaction regions (CIRs) alone could have produced them. While this statement is much weaker than concluding that CIR structure was not present during the Maunder Minimum, at least an inference can be drawn that it may not have been.

2.3. Cosmic Ray Fluxes inferred from Cosmogenic Records

Cosmogenic isotopes are rare isotopes created when a high-energy cosmic ray interacts with the nucleus of an atom in the Earth's atmosphere. The two principal products are ^{10}Be and ^{14}C. Here, we focus principally on the former, since it is more directly relatable to cosmic ray intensities (Steinhilber et al. 2012). High-energy galactic cosmic ray particles impact atmospheric nitrogen or oxygen, producing ^{10}Be, which then become

attached to aerosols. Depending on where the ^{10}Be is produced it may take from weeks (troposphere) to a year or two (stratosphere) before being deposited in the polar ice caps. Since climate/precipitation effects can modulate the ^{10}Be concentrations within the ice, care must be taken when interpreting the records as a measure of cosmic ray intensities. The general consensus, however, is that ^{10}Be records provide, primarily, a measure of production rates (Usoskin 2008).

In panel (c) of Figure 1 we show the ^{10}Be record as reported by Berggren et al. (2009). The individual circles are yearly measurements of concentration. The black/blue curve represents an 11-year running average. We note several points. First, the solar cycle is clearly seen, particularly after 1895 (the beginning of the "Gleissberg" minimum). Second, the absolute concentration varies by a factor of ~ 2.5 over the 400-year interval. Third, the three established minima (Maunder, Dalton, and Gleissberg) all coincide with local peaks in concentration. Fourth, a striking feature is that, unlike the Sunspot record, the Maunder minimum as viewed through $10^{B}e$ was not steady. The Be-10 data steadily increased from 1.75×10^4 atoms/g to over 3×10^4 during the 70-year interval. Thus, at least from a cosmic ray perspective, the Maunder minimum period was a period of evolution, not constancy.

We might reasonably infer then that if, as the record suggests, the CR flux increased by almost a factor of two, this suggests a commensurate decrease in the strength of the interplanetary magnetic field. In fact, the relationship between CR flux and the strength of the IMF is considerably more complicated (Usoskin 2008). We will return to this point in Section 2.5, where we consider the modulation potential.

The ^{10}Be record also calls into question the idea that the Maunder Minimum interval is substantially the same as the 2008/2009 minimum. In particular, the recent minimum is a snapshot of the Sun in time, whereas, as we have argued here, the Maunder minimum was an evolving configuration: If the recent minimum is related to the Maunder Minimum,

to which part is it associated with? Presumably, it would be the beginning, since we have not yet witnessed the 70 years of little-to-no sunspots or the continual increase in cosmic ray fluxes. We conclude then, that at best, the 2008/2009 minimum may turn out to be the first minimum that defined the start of a new grand minimum.

Finally, in panel (d) of Figure 1 we show yearly averages of the ^{14}C record as reported by Reimer et al. (2004). Again, a large value of ^{14}C suggests a stronger flux of cosmic rays, which in turn suggests a lower interplanetary field, possibly in conjunction with a relatively flat HCS. We note the almost monotonic increase from 1600 until shortly after 1700, consistent with the ^{10}Be record. Between then and until 1955, it appears to generally decrease, except for two 'recoveries' when it rises. The first occurred in $\sim$ 1800 and the second, shortly before $\sim$ 1900, coinciding with the Dalton and Gleissberg minima. Above-ground nucear tests began in 1955 rendering the time series from this point forward useless for present purposes. In fact, secular variations after $\approx$ 1900 are probably dominated by the anthropogenic effects of fossil fuel burning (Usoskin 2008).

Comparing the ^{14}C and ^{10}Be profiles, we note that, on the largest scales, they convey a similar trend for the inferred flux of cosmic rays. The three grand minima (seen as maxima in these records) are approximately co-temporal and the general variations about some reference point, say 1600, are reasonably matched. One notable exception is that while the peak ^{10}Be values during the Maunder and Dalton intervals match one another, they are substantially different in the ^{14}C record, perhaps the result of being superimposed on a monotonic decrease from 1700 until at least 1955.

From this, we conclude that the cosmic ray flux was larger during the Maunder Minimum than at any time over the last 400 years. Moreover, the flux of particles systematically increased during the 70-year interval, suggesting that the minimum was only "flat" only from the perspective of sunspots. If anything, the true "Maunder minimum"

was not an interval, but a point in time that occurred circa 1700.

2.4. Eclipse "Observations"

Observations of eclipses during the Maunder Minimum are strongly suggestive, but not conclusive, that the structured corona observed in modern times during eclipses disappeared (Eddy 1976). Here, we build upon, and add to the evidence compiled by J. Eddy. As he noted, of the 63 possible solar eclipses known to have occurred between 1645 and 1715, only eight passed through Europe, and, of those four (1652, 1698, 1706, and 1708) were captured by reports sufficiently detailed to be of use for this study.

Dr. John Whybard gave an account of his, and that of the vice-prefect's observations of the 1652 solar eclipse in Carrickfergus, located in County Antrim, Northern Ireland (Wing 1656). He stated that the corona "had a uniform breadth of half a digit, or a third of a digit at least, that it emitted a bright and radiating light, and that it appeared concentric with the sun and moon when the two bodies were in conjunction."

As reported by Grant (Grant 1852), MM. Plantade and Capies observed the eclipse of 1706 at Montpellier, located on the south coast of France, in a way that was "clearer and more precise than any other that had been hitherto recorded." They observed that "as soon as the sun was totally eclipsed, there appeared around the moon a very white light forming a kind of corona, the breadth of which was equal to about 3". Within these limits the light was everywhere equally vivid, but beyond the exterior contour, it was less intense, and was seen to fade off gradually into the surrounding darkness, forming an annulus around the moon of about 8 degrees diameter."

Both sets of reports describe a structureless corona composed of a ring of light circumscribing the entire moon. Had the Sun displayed a dipolar or quadrupolar

configuration, such as any of the eclipses viewed in, say, the last century, we might have expected the observers to note this fact.

The eclipse of 1715, which was well observed from London, however, lays some doubt on this inference. Halley himself reported that there "appeared a luminous ring around the moon as on the occasion of the eclipse of 1706," suggesting at least a qualitative similarity between the two events. R. Cotes, on the other hand wrote "besides this ring, there appeared also rays of a much fainter light in the form of a rectangular cross...The longer and brighter branch of this cross lay very nearly along the ecliptic, the light of the shorter was so weak that I did not constantly see it." Eddy (1976) interpreted the longer, brighter branch to be a description of a solar minimum streamer belt configuration and the shorter branch to be polar plumes. The discrepancy between these two accounts raises several issues. First, it is possible that earlier accounts failed to acknowledge that there was an underlying structure. Or, second, that the structured K-corona had returned to the Sun by the time of the 1715 eclipse.

The eclipse of 1766, which was observed "in the Southern Ocean by the persons on board the French ship of war the Comte d'Artois," provides clear evidence that "normal" solar conditions had returned. Although totality only lasted some 53 seconds, the observers noted "a luminous ring about the moon, which had four remarkable expansions situate at a distance of 90 [degrees] from each other." From this we can infer that a quadrupolar streamer structure was visible. Additionally, it bolsters support for the interpretation that had this structure been present in 1652, it would have been noted.

Finally, we remark that during the eclipses of 1652, 1698, 1706, and 1708, the corona was described as "dull or mournful," and often as "reddish," which Eddy (1976) suggested might describe how the zodiacal light component (i.e., the F-corona) might look to an observer in the absence of a K-corona.

In summary then, we conclude that: (1) the corona during the Maunder Minimum was likely featureless, at least to the extent that it was not commented on; (2) the coronal light that was present was "reddish" and (3) coronal features returned sometime between 1708 and 1766. Given the qualitative nature and questionable reliability of the reports, we must assign large uncertainties to these inferences.

2.5. Cosmic Ray Modulation Potential

Variations in cosmogenic radionuclide records, and, in particular ^{10}Be and ^{14}C, are believed to provide a measure of solar activity. To a rough approximation, their values indicate the flux of cosmic rays impinging the upper atmosphere. However, the transport and deposition mechanisms for both species is relatively complex and quite different from one another, meaning that interpretation does not come without important caveats. Usoskin (2008) has explored – in detail – the various processes that affect cosmogenic records.

A number of both empirical and physics-based models have been developed to recover unbiased estimates of "solar activity." Here, we focus on the so-called modulation potential, ϕ. As suggested by its name, ϕ is intended to capture the variability in the observed cosmic ray flux in the vicinity of Earth. Because these fluxes are modulated on a global scale, ϕ is a global heliospheric quantity, capturing the physical processes of: (1) diffusion of particies due to scattering; (2) convection in the solar wind; (3) adiabatic losses; and (4) particle drifts. The following empirical estimate for ϕ provides an intuitive way to understand it:

$$\phi = \phi_o + \phi_1 \left(\frac{F}{F_o} \right)^{1+\frac{\alpha}{\alpha_o}} (1 + \beta p) \tag{1}$$

where F is the open solar flux, α is the tilt angle of the HCS, and p is the global magnetic polarity; $p = 1(-1)$ for positive (negative) polarity periods. Best fit values for the

constants are: $\phi_o = 150$MV, $\phi_1 = 86$MV, $F_o = 2.5 \times 10^{14}$Wb, $\alpha_o = 91°$, and $\beta = -0.03$ (Alanko-Huotari et al. 2006).

From Equation (1), we can appreciate that during solar minimum periods, when $\alpha \to 0°$, the modulation potential is linearly proportional to the open flux in the heliosphere. During elevated periods of activity (and in the extreme that $\alpha \to 90°$) the modulation potential is more sensitive (up to the square) of the open flux. Intuitively, this makes sense: During periods of higher activity, as the heliospheric magnetic field strength increases and the latitudinal extent of the HCS broadens there is a larger barrier for cosmic rays to impact the Earth. In contrast, when the HCS becomes flat, and the field strength reduces, the structure of the solar wind provides no impediment to the propagation of these particles. Of the two parameters, since α varies between 10° and 90° every 11 years, it doesn't impact ϕ as much as F, which varies by more than a factor of two. Moreover, α must oscillate between these extremes every cycle, and cannot drift beyond them on longer times scales as can F. Therefore, we conclude that long-term variations in ϕ likely represent changes in the large-scale heliospheric magnetic field strength.

Armed with this simplified picture, we can now interpret several reconstructions of the modulation potential shown in Figure 2. The solid colored lines show various estimates of ϕ using both ^{10}Be and ^{14}C records. The black solid line is an eleven-year running mean of monthly averages (black points) of ϕ derived from neutron monitor measurements. The approximate match between the cosmogenic records and the neutron monitor measurements gives us some confidence that present day values can be – at least roughly – compared with historical estimates, particularly during the deepest portion of the Maunder Minimum ($\approx$ 1700). However, more important than the absolute values, is the variability in the cosmogenic data between 1600 and 2000. If we assume that, to first order, ϕ is providing a proxy for the strength of the heliospheric magnetic field, then its strength during the

Maunder Minimum was as much as 500/50 = 10 times lower than it was during the decade beginning in 2000. Additionally, the field strength during the early 1600's, which, it could be argued was the beginning of a long term, monotonic decrease in field strength, is approximately the same as the inferred field strength today, reinforcing the suggestion by Lockwood & Owens (2011) that we may be entering a grand solar minimum, similar to the Maunder interval.

These profiles also promote the idea that the Maunder minimum was not an extended interval of constant inactivity, as might be inferred from the sunspot record, but a progressive drop, culminating in an absolute minimum (what we have dubbed "the day the Sun stood still") roughly located at 1700.

3. Candidate Scenarios for the Sun's Photospheric Magnetic Field during the Maunder Minimum

The Sun's photosphere provides a convenient boundary from which to base our calculations. First, the photospheric magnetic field is well observed by both ground-based and space-based solar observatories. Second, the transition from a flow-dominated to a magnetic field-dominated environment occurs at the photosphere. In principle then, assuming that all of the salient physical processes are included in the models, and that the model results are not strongly dependent on the values of free parameters (i.e., coefficients in the formulation of the relevant physics that are not well constrained), specification of the photospheric magnetic field should be sufficient to reconstruct the global structure of the corona and inner heliosphere. Such models are frequently applied to data from the modern era driven by the observed photospheric magnetic field, in an effort to understand the large-scale structure of the corona and inner heliosphere, and generally match the observed large-scale structure of the inner heliosphere (e.g., Riley et al. (2012b,a)).

The distribution of magnetic field in the photosphere during the Maunder minimum, however, is subject to considerable speculation. We have reasonably reliable evidence that few, to no sunspots were observed during this period, suggesting the absence of active regions. Theoretically, several studies have speculated on various aspects of the Maunder Minimum solar field. Schrijver et al. (2011) argued that small-scale fields associated with ephemeral regions must have persisted during even the deepest portion of the interval. Mackay (2003) proposed that the Maunder Minimum must have commenced at, or near solar minimum: Had it started at solar maximum, there would have been no reversal of the polar fields, in apparent conflict with evidence that the solar cycle continued to operate during this 70-year period. Thus, one approach to deducing the photospheric field during this interval is to construct a range of possible scenarios, at least acknowledging these constraints, and test their predictions against the available, albeit limited "observations."

We can safely discount the extreme possibility, raised (but not necessarily advocated) by Parker (1976), that the entire visible magnetic field disappeared. While this would provide an obvious means for removing all sunspots, we know: (1) that there were very occasional sunspots during the Maunder interval; (2) there were occasional geomagnetic storms; and (3) at least the suggestion of a solar cycle still operating during this interval. The continued, sporadic appearance of sunspots suggests that magnetic flux continued to emerge through the photosphere, albeit at a much lower rate. The occasional geomagnetic storms suggests a continued magnetic connection between the solar surface and Earth's magnetosphere. And, the maintenance of a solar cycle suggests that the field did not "extinguish" itself, which, from a theoretical perspective, would be difficult to envisage.

Thus, we suggest that the most radical scenarios for the Maunder Minimum photosphere may have contained only small-scale ephemeral flux, random in amplitude and position, but substantially less (say, one third to an order of magnitude) than currently-observed

ephemeral regions. Figure 3(e) and (f) summarize a photosphere composed of only parasitic polarity of strength ±10G and ±3.3G, respectively. The former was chosen to match the observed flux (at this resolution) during 2008, and the latter is simply a 1/3 scaling. Evolutionarily, we might anticipate that this state was arrived at slowly as the polar fields decayed, not being replaced by poleward-migrating flux from sunspots, which had disappeared, Thus, this might represent the state of the Sun late in the Maunder Minimum interval.

At the other end of the spectrum, the most conservative scenario would be that the Maunder minimum period was no different than the recent minimum of 2008/2009, as suggested by Schrijver et al. (2011) (Figure 3(a)). If substantiated, this is an appealing result because all of the modern era measurements, modeling, and inferences could be applied to better understand, and constrain the Maunder interval.

Between these two extremes, we consider several alternatives. In the first (Figure 3(b)), we construct a 2008/2009-like configuration by superimposing an axial dipole of strength 3.3G on top of a parasitic polarity distribution with peak amplitude of ±3.3G. In the second, (Figure 3(c)), we consider a dipole only, with strength 3.3G. The third scenario reproduces case (b), except that the large-scale dipole is reduced to 1G.

These six scenarios represent a wide possible array of configurations for the distribution of flux in the photosphere that may have existed during the Maunder Minimum.

4. Global MHD Modeling

A global MHD model of the solar corona and inner heliosphere can provide a unique and powerful way to "self-consistently" link the disparate observations discussed in Section 2 and assess the likelihood that any of the scenarios discussed in Section 3 are consistent or in

conflict with these observations. The model we describe in the following sections contains the key elements that: (1) The primary driver is the photospheric magnetic field; and (2) the heating of the corona is a function only of the photospheric magnetic field strength. Thus, the magnetic and emission properties of the corona are coupled, and we can, at least in principle, apply the model to epochs with significantly different properties.

4.1. Model Description

The MHD approximation is appropriate for large-scale, low-frequency phenomena in magnetized plasmas such as the solar corona. Using the photospheric magnetic field as the primary driving boundary condition, as described in Section 3, we can attempt to reproduce the Sun's magnetic and emission properties during during the Maunder Minimum by solving the following set of viscous and resistive MHD equations:

$$\nabla \times \mathbf{B} = \frac{4\pi}{c}\mathbf{J}, \tag{2}$$

$$\nabla \times \mathbf{E} = -\frac{1}{c}\frac{\partial \mathbf{B}}{\partial t}, \tag{3}$$

$$\mathbf{E} + \frac{\mathbf{v} \times \mathbf{B}}{c} = \eta \mathbf{J}, \tag{4}$$

$$\frac{\partial \rho}{\partial t} + \nabla \cdot (\rho \mathbf{v}) = 0, \tag{5}$$

$$\frac{1}{\gamma - 1}\left(\frac{\partial T}{\partial t} + \mathbf{v} \cdot \nabla T\right) = -T\nabla \cdot \mathbf{v} + \frac{m}{2k\rho}S \tag{6}$$

$$\rho\left(\frac{\partial \mathbf{v}}{\partial t} + \mathbf{v} \cdot \nabla \mathbf{v}\right) = \frac{1}{c}\mathbf{J} \times \mathbf{B} - \nabla(p + p_w) + \rho \mathbf{g} + \nabla \cdot (\nu \rho \nabla \mathbf{v}), \tag{7}$$

$$S = (-\nabla \cdot \mathbf{q} - n_e n_p Q(T) + H_{\rm ch}), \tag{8}$$

where $\mathbf{B}$ is the magnetic field, $\mathbf{J}$ is the electric current density, $\mathbf{E}$ is the electric field, ρ, $\mathbf{v}$, p, and T are the plasma mass density, velocity, pressure, and temperature, $\mathbf{g} = -g_0 R_\odot^2 \hat{\mathbf{r}}/r^2$ is the gravitational acceleration, η the resistivity, and ν is the kinematic viscosity. Equation (8) contains the radiation loss function $Q(T)$ as in Athay (1986), n_e and n_p are the electron

and proton number density (which are equal for a hydrogen plasma), $\gamma = 5/3$ is the polytropic index, $H_{\rm ch}$ is the coronal heating term (see below), and $\mathbf{q}$ is the heat flux.

For the present study, we have used a grid of $151 \times 180 \times 360$ points in $r \times \theta \times \phi$. The grid resolution is nonuniform in r with the smallest radial grid interval at $r = R_\odot$ being ~ 0.33 km. The angular resolution in θ and ϕ is 1°. A uniform resistivity η was used, corresponding to a resistive diffusion time $\tau_R \sim 4 \times 10^3$ hours, which is much lower than the value in the solar corona. This is necessary to dissipate structures that cannot be resolved which are smaller than the cell size. The Alfvén travel time at the base of the corona ($\tau_A = R_\odot/V_A$) for $|\mathbf{B}| = 2.205$ G and $n_0 = 10^8$ cm^{-3}, which are typical reference values, is 24 minutes, and so the Lundquist number $\tau_R/\tau_A \approx 1 \times 10^4$. A uniform viscosity ν is also used, corresponding to a viscous diffusion time τ_ν such that $\tau_\nu/\tau_A = 500$. Again, this value is chosen to dissipate unresolved scales without substantially affecting the global solution. Our model includes a chromosphere and transition region (Lionello et al. 2009).

4.2. Coronal Heating

Global MHD models of the solar corona and inner heliosphere have demonstrated their ability to reproduce the essential features of a range of measurements and observations during the space era (e.g., (Riley et al. 2012b,a)). A crucial aspect and limitation of current capabilities concerns the physical mechanisms that heat the corona. While it is generally believed that it must involve the conversion of magnetic energy into heat, it is not clear how this transformation takes place. One scenario involves the dissipation of high-frequency waves, while another relies on the rapid release of energy built up from slow photospheric motions (e.g., Lionello et al. (2009)). Phenomenologically, it is well known that magnetic flux and X-ray radiance are linearly correlated over many orders of magnitude (Fisher et al. 1998; Pevtsov et al. 2003; Riley et al. 2009).

In this study, we take the pragmatic but necessary position of specifying the heating as a function of magnetic field strength. Specifically, we assume that the heating of the corona takes the following form:

$$H = H_{\rm QS} + H_{\rm AR} \tag{9}$$

$$H_{\rm QS} = H^0_{\rm QS} f(r) \frac{B_t^2}{B(|B_r| + B_r^c)} \tag{10}$$

$$H_{\rm AR} = H^0_{\rm AR} g(B) \left(\frac{B}{B_0}\right)^{1.2} \tag{11}$$

where: $B_t = \sqrt{B_\theta^2 + B_\phi^2}$, $H^0_{\rm QS} = 1.18 \times 10^{-5}$ erg/cm^{3}s, $B_r^c = 0.55$ G, $H^0_{\rm AR} = 1.87 \times 10^{-5}$ erg/cm^{3}s, and $B_0 = 1$ G, $f(r) = \exp\left(-\frac{r/R_\odot - 1}{0.2}\right)$, and $g(B) = \frac{1}{2}\left(1 + \tanh\frac{B-18.1}{3.97}\right)$.

Although these functions are *ad hoc*, importantly, they depend only on the strength of the magnetic field, and hence, provided that coronal heating too depends only on field strength, should be applicable to a range of values even outside those that have been observed during the space era. Thus, by demonstrating that the model can reproduce observations during the space era, and requiring that the heating profiles depend only on the magnetic field, that is, that there are no additional free parameters, we have some confidence that the heating profiles should be applicable when applied to more extreme conditions.

4.3. Computation of the Open Magnetic Flux

Open solar magnetic flux can be practically defined as that flux which threads through some reference sphere, say, the fast-mode critical point, or even 1 AU. Assuming

further that, on sufficiently long temporal scales, this flux is independent of position in the heliosphere, as suggested by Ulysses observations (Smith & Marsden 2003), in-situ measurements of the interplanetary magnetic field, B_{IMF}, are a proxy for the open flux. Multi-solar cycle measurements of B_{IMF} demonstrate that the open flux roughly doubles between solar minimum and solar maximum. Owens et al. (2006), Riley et al. (2007) and Schwadron et al. (2010) have argued that the measured flux at 1 AU consists of a relatively constant background flux, with an additional contribution from CMEs, which at solar maximum can be as large as the background level.

Therefore, under solar minimum conditions, and for timescales longer than a solar rotation, the average open flux computed from the MHD model should match estimates for $|B_r^{IMF}|$ as measured by in-situ spacecraft or via indirect estimates from cosmogenic records. In particular, following Wang & Sheeley (1995), we can estimate the magnitude of the radial interplanetary magnetic field at Earth from the MHD solution as:

$$|B_r^E| = \frac{|\Phi_{open}|}{4\pi r_E^2} = \frac{1}{4\pi}\Big(\frac{R_s}{215R_\odot}\Big)^2 \int |B_r(R_s,\theta,\phi)| d\Omega \tag{12}$$

where ϕ denotes longitude, $R_\odot$ radius of the Sun, R_s is the radius of the source surface, typically $2.5R_\odot$, r_E is the distance of the Earth from the Sun (1 AU), and the solid-angle integral is computed over a sphere at the source surface.

4.4. Model Results

We used the six magnetograms described in Section 3 to compute MHD model solutions of the solar corona from 1 to 30 R_S. The resulting magnetic field configurations are shown in Figure 4. The same starting points were used in each panel, corresponding to a mesh resolution of 10° in latitude and longitude. We note several points. First, a relatively clear

streamer belt configuration can be discerned for cases (a) - (d): Field lines emanating from the polar regions extend into interplanetary space and remain open. Those straddling the heliospheric equator tend to be closed. Second, there is a qualitative decrease in the amount of open flux in moving from (a) to (f), at least based on the number of field lines drawn. Third, there is a net decrease in the organization of field lines from (a) to (f) (except for (c), which displays perfect axial symmetry). This is particularly true for comparisons between (a)-(d) and (e)-(f), the latter showing no obvious axis of symmetry. Interestingly, (d), although displaying axial symmetry, appears to be tilted substantially with respect to the rotation axis, presumably because of the presence of a coherent feature in the parasitic polarity.

For each solution, we computed the open magnetic flux, as defined by Equation (12). These are summarized in Table 1. Our "standard run," CR 2085, produced an open flux of 1nT at 1 AU. Scenario (b) results in the largest amount of open flux (2.4 nT), then scenarios (b) through (f) yield progressively less flux. The largest proportional change occurs for (e) to (d) – a factor of 4.1, followed by the change from (f) to (e) – a factor of 3.6. The value computed for CR 2085 (scenario (a)), is lower than estimates made using near-Earth spacecraft (and earlier observations from Ulysses). However, the relative variations in open flux between models and observations has been shown to match well (Wang & Sheeley 1995). Stevens et al. (2012) have investigated the known deficit in the open flux produced by the models, suggesting that a better estimate of some of the model parameters (e.g., coronal base temperature) may resolve the difference. Additionally, more recent analysis by Linker et al. (2012) suggests that current synoptic maps may be underestimating the polar field strengths, which would lead to a systematic reduction in the model estimates for the open flux. For our purposes, assuming that the relative differences are reasonably accurate, scenarios (e) and (f) predict reductions over 2008 conditions of a factor of ≈ 12.5 and ≈ 3.4, respectively. Additionally, it should be noted that the 2008 time period we are

comparing to represents a somewhat unique interval where the fields were lower by a factor of 1.6 over the previous space era minima (Smith & Balogh 2008), and general solar activity was estimated to be the lowest it had been in the last century (e.g., Riley et al. (2011)). The range bracketed by scenarios (e) and (f) is consistent with the difference between the curves in Figure 2 when contemporary values are compared with those in 1700.

We next consider the structure of the corona in white light that these scenarios suggest. In Figure 5, we have computed the simulated polarized brightness (pB) for each solution. These were constructed by integrating the plasma along the line of sight with a suitable weighting function (Billings 1966). We have found that the model usually matches observed white light images both from spacecraft and ground-based observations during eclipses (Riley et al. 2001; Mikić et al. 2007; Riley 2010; Riley et al. 2012b). Scenario (a), which represents the corona during the last solar minimum displays the typical mid- and low-latitude streamer structure we expect during the declining phases and solar minimum. The recent minimum was unique in that there were a larger number of pseudo-streamers present than during the previous (1996) minimum, which led to a broader and more structured "belt" of brightness around the equator (Riley & Luhmann 2012). The presence of unipolar polar fields is clearly seen by the dark regions over both poles. Scenario (b), which represents an idealization of scenario (a) by removing any large-scale active regions, as well as scenario (c) for which the parasitic polarity has been removed, present similar pictures. The closed, dipolar fields bracketing the equator trap plasma that scatters photons to the observer while the polar, open field regions retain only a tenuous outwardly streaming flow of plasma that cannot be easily seen in white light. Scenarios (e) and (f) are both much darker and do not display any axial symmetry. It is likely that scenario (f) would not be visible to the naked eye, especially if contrasted with the relative brightness of the preceding partial eclipse. Scenario (e) is marginally more visible, and appears to show some structure. Whether or not this would be reported, or whether only the more

dominant effect of a "halo" or "annulus" would be noted by observers of the time is unclear. Scenario (d), which in some sense was designed to bridge the gap between (a)-(c) and (e)-(f) by reducing the dipole strength by a factor of 3.3, clearly shows a streamer-belt-like configuration. We conclude from these images that had scenarios (a) through (d) been in effect during the Maunder Minimum, observers would probably have noted the existence of structure within the white-light corona.

The white light we observe from the solar corona is made up of two primary components: the K (kontinuierlich) and F (Fraunhofer) corona. The K-corona is created by sunlight scattering off free electrons, while the F-corona is created by sunlight scattering off dust particles. Close to the Sun, the K-corona dominates; however, beyond $\approx 3R_S$ (the precise number depending sensitively on the point of observations and solar conditions), the brightness of the F-corona exceeds that of the K-corona (Koutchmy & Lamy 1985). Here, it is important to differentiate between brightness, B, and polarized brightness, pB: While coronagraphs (and MHD simulation results) often display images of pB, at visible wavelengths, the polarization of the F-corona is nearly zero, hence it it not observed in images of pB, even at larger distances. But, more importantly, our eyes 'see' B. Thus, to directly relate our simulation results to the reports of eclipses during the Maunder Minimum, we should limit ourselves to B.

Figure 6 is an estimate of the F-corona as it might have looked during the Maunder Minimum using the formulae by Koutchmy & Lamy (1985). In fact, this picture is indistinguishable from how it would appear today, given that the dust giving rise to it was formed from asteroid collisions and cometary activity, for which the timescales are much longer. We also have taken the liberty of using a red color table based on work suggesting that there is a strong reddening of the spectrum (see Koutchmy & Lamy (1985) and references therein). It is, however, by no means certain that if the K-corona disappeared

completely, that the remaining F-corona would appear as red as shown here. The main point to make is that the F-corona shows no discernible structure with respect to position angle. Although there is a slight variation between the equator and pole, this would be imperceptible to the naked eye. An observer fortunate enough to witness the F-corona directly would report a smooth annulus or halo surrounding the Sun, possibly reddish in color.

To make a direct comparison between the F- and K-corona during the Maunder Minimum, we computed simulated total brightness (B) images, analogous to those shown in Figure 5. From these, we extracted radial traces taken through the solar equator for each scenario, and compared them with the F-corona brightness estimates discussed above. These are shown in Figure 7. We remark on the clear separation between scenarios (a)-(d) and (e)-(f). The former dominate over the F-corona (red) at least out to $2R_S$. The latter, however, are dominated by the F-corona by $1.3R_S$. Comparison with Figure 5 suggests that the range between $1.3R_S$ and $2R_S$ is precisely where coronal structure manifests itself in white-light eclipse observations. Given the idealizations and approximations employed to arrive at this result, it is quite remarkable that such a clear delineation occurs. Based on these results, then, we would anticipate that an eyewitness to scenarios (e) or (f) would not observe any structure of the true (K-) corona because it would be obscured by the (potentially red) and structureless F-corona. On the other hand, an observer of scenarios (a)-(d) would likely see helmet streamer, pseudo streamer, coronal hole, and plume structure before being washed out by the F-corona.

4.5. Bayesian Analysis

Our analysis, thus far, has produced only qualitative inferences on the likely state of the corona during the Maunder Minimum. However, these are subjective, in the sense that

two reasonable people could disagree. For example, while the reports of a "red erie glow" during some of the eclipse observations is suggestive of the presence of an F-corona, one could argue that these were the result of local atmospheric effects, or even sensitivities unique to the observer. In an attempt to incorporate various types of evidence to arrive at a more reliable estimate for the probability that a given hypothesis is true, based on various pieces of evidence, we can invoke a Bayesian-type analysis. Although its application is sometimes criticized for being itself subjective, it does provide a robust methodology, and it is particularly well suited for comparing exclusive ideas. In our case, scenarios (a) - (f) have captured two distinct ideas. First, that the Maunder Minimum Sun was like that in 2008/2009 (the "2008 Sun") ((a) - (d)). And second, that the Sun consisted exclusively of parasitic polarity, with no large-scale dipole component (the "ephemeral-only" Sun.)

Using Bayes's theorem, we can write:

$$\frac{P(H_1|\epsilon)}{P(H_0|\epsilon)} = \frac{P(H_1)}{P(H_0)} \frac{P(\epsilon|H_1)}{P(\epsilon|H_0)} \tag{13}$$

where the fraction on the left-hand side is the posterior odds, the first fraction on the right-hand side is the prior odds, and the second fraction on the right-hand side is the likelihood ratio. It is worth considering these terms in more detail. $P(H_1|\epsilon)$ is the conditional probability that hypothesis H_1 is true, given evidence ϵ. Thus, the posterior odds is the amount by which hypothesis H_1 is more likely than H_0, given the evidence ϵ. The power of Bayes's theorem lies in the fact that the posterior odds are calculated from the terms $P(\epsilon|H_1)$ and $P(\epsilon|H_1)$, that is, the probability that the evidence would have arisen given under each of the competing scenarios. In fact, for a set of n pieces of evidence, we can generalize Equation (13) as follows:

$$\frac{P(H_1|\epsilon)}{P(H_0|\epsilon_1, ..., \epsilon_n)} = \frac{P(H_1)}{P(H_0)} \prod_{i=1}^{n} \frac{P(\epsilon_i|H_1)}{P(\epsilon_i|H_0)}. \tag{14}$$

Turning to the specific case of distinguishing between the "ephemeral Sun" and "2008 Sun" scenarios, if we assume that these are mutually exclusive hypotheses, and that only two possibilities exist, we need only construct the likelihood ratios for each piece of evidence, multiply them together and with our prior odds, to estimate the posterior odds.

In table 2, we have listed each piece of evidence that might support either the conclusion that the Maunder Minimum Sun was "2008-like" or "ephemeral-like" based on our analysis in Section 2. If we further assume that the evidence distinguishes only between the two ideas, then $P(\epsilon|H_1) + P(\epsilon|H_1) = 1$. Thus, if the evidence does not distinguish between either scenario, we might infer that $P(\epsilon|H_1) = P(\epsilon|H_1) = 1/2$. On the other hand, if the evidence favors the ephemeral Sun idea, which most do, $P(\epsilon|H_1) > P(\epsilon|H_1)$. While it is not possible to deduce precise values for $P(\epsilon|H_1)$ or $P(\epsilon|H_1)$ for any of these observations, the key point is that because they are multiplicative, even modest individual biases in favor of one hypothesis over the other can result in a substantial shift in the posterior odds ratio. For example, if each piece of evidence in Table 2 favored one hypothesis over the other in the ratio $\frac{0.6}{0.4}$, then, because the last two rows would cancel one another, the "ephemeral Sun" scenario would be $(\frac{0.6}{0.4})^5 \approx 7.6$ times more likely to be correct than the "2008 Sun." As we noted earlier, however, reasonable minds will disagree. The main point though is that the weight of the evidence supports the "ephemeral-only" Sun, and not the 2008/2009 Sun picture. Only one piece of evidence distinguishes between the two scenarios in favor of the latter, while six, arguably independent pieces of evidence favor the former.

5. Discussion

Our analysis appears to safely rule out the idea that the Maunder Minimum Sun was substantially the same as the recent 2008/2009 minimum (Svalgaard & Cliver 2007; Schrijver et al. 2011; Wang & Sheeley 2013) or that coronal magnetic fields disappeared

entirely. The continued modulation of cosmic rays, including the inferred presence of a 22-year cycle, as well as albeit modest auroral activity, requires both some magnetic field and a continuing dynamo process. The lack of any observations reporting coronal structure, the possible presence of an F corona, and likely decrease in the strength of the IMF also contradict the idea that the Maunder Minimum Sun was no different than in 2008/2009. It is worth noting that Schrijver et al. (2011) and Svalgaard & Cliver (2007) based their conclusions on assumptions or hypotheses, which were extrapolated back to the Maunder Minimum Interval. Schrijver et al. (2011) argued that there is a minimum state, or "floor" in solar activity, associated with small-scale magnetic bipoles (i.e., what we have called ephemeral regions). However, they did not address whether or not polar coronal holes would have been present during the Maunder Minimum. Svalgaard & Cliver (2007) posited a similar "floor" but this time, in terms of the strength of the interplanetary magnetic field. This was based on empirical evidence from the minima of 1976, 1986, and 1996. The floor, however, had to be lowered as the 2008/2009 minimum dropped below the value predicted for it.

Table 2 summarizes the key observations we have analyzed here. It reduces the interpretation of these observations to two major candidates: the '2008 Sun' and the 'Ephemeral Sun.' The ephemeral Sun picture is generally consistent with all observations - or at least with the consensus interpretation of them. On the other hand, the 2008 Sun is inconsistent with all, except for the continued modulation of cosmic rays. Of course, arguments can be made that the observations are inaccurate, imprecise, or that their interpretation is incorrect. However, from a purely statistical point of view, we are led to the conclusion that the ephemeral Sun is significantly more consistent with the observations.

An important point to make is that the Maunder minimum was not a steady period of inactivity. Instead, it is likely that there was a general progression to a progressively deeper

configuration during the 70-year period. Therefore, it may be more reasonable to compare the 2008/2009 solar minimum with the initial descent into the Maunder minimum; however, it is unlikely that the last 5-10 years looked anything like the recent minimum. Thus, we suggest that the Sun's magnetic field continued to evolve during this interval and posit that this evolution is best represented by an ever-decreasing surface field, and, in particular, the gradual decay of the polar fields. These polar fields are the dominant source of the open flux permeating the heliosphere and modulating the flux of cosmic rays hitting Earth's magnetosphere. By 1700, the point in the Maunder Minimum that we associate with "the day the Sun stood still" likely consisted of only small-scale parasitic polarity field, with virtually no large-scale dipolar component, i.e., no unipolar fields.

Our results are in apparent conflict with several numerical studies. Mackay (2003) used a magnetic flux transport model to consider the possible surface magnetic field configurations that may have been present during the Maunder minimum. They concluded that if the grand minimum started at solar cycle minimum, then a large amount of unipolar flux may have persisted in the polar regions of the Sun, whereas, if the minimum had started at solar maximum, there may have been little-to-no large scale magnetic flux on the Sun. Additionally, Wang & Sheeley (2013) argued that an "ephemeral only" Sun was not possible because the inferred interplanetary magnetic field strength would be inconsistent with estimates based on the ^{10}Be record. Their approach for estimating the open flux that a distribution of randomly orientated small-scale dipoles would produce, however, rested on a magneto static extrapolation of the large-scale residual field produced by them. Importantly, it did not take into account the fact that small loops would be heated, expand, and potentially open up into the solar wind; a result that could only be revealed using an MHD approach, as described here. In fact, our results suggest that an ephemeral-only Sun is capable of supplying an open flux that may be 1/10 to 1/3 of the value measured in 2008/2009, clearly consistent with the cosmogenic records.

Our invocation of Bayesian methodology to argue that the "ephemeral-only" Sun is strongly favored may seem awkward. In fact, the case for the the "ephemeral-only" Sun can be made simply by scanning Table 2. However, the Bayesian approach provides two advantages. First, it emphasizes that the individual pieces of evidence combine in a multiplicative fashion to support one hypothesis over the other. Second, it provides a conceptual framework for understanding the fallacy of arguments that seek to promote an alternative hypothesis by attacking the credibility of the evidence supporting the former. For example, consider observations of eclipses during the Maunder minimum. While one can argue that there may have been omissions or even biases in the reports, this only goes to the credibility of the evidence, that is, a measure of the error bars. The most probable interpretation remains that these observations tend – even if only slighty – to favor the "ephemeral-only" picture, and they actively refute the "2008/2009" scenario. As with error analysis in general, we derive the best estimate of the parameter by multiplying the individual parameters together, and then, we add the relative individual errors. We may conclude that the errors are large enough that they admit either hypothesis; however, our conclusion remains that the most likely scenario is the "ephemeral-only" Sun.

In closing, our analysis of the available observations during the Maunder Minimum, together with their interpretation within the context of global MHD model results strongly suggests that this period was unlike anything we have observed in recent times. As such, it once again "opens the door" for the possible connection between the Maunder Minimum and the little-ice age.

This work was motivated by discussions during the two ISSI (International Space Science Institute) team workshops on "Long-Term Reconstruction of Solar and Solar Wind Parameters," which occurred in May, 2012 and 2013. PR gratefully acknowledges the support of NASA (Causes and Consequences of the Minimum of Solar Cycle 24

program, LWS Strategic Capabilities program, Heliophysics Theory Program, and the STEREO IMPACT team) and NSF (Center for Integrated Space Weather Modeling (CISM) program).

REFERENCES

Owens, M. J., Merkin, V. G., & Riley, P. 2006, J. Geophys. Res., 111, A03104

Alanko-Huotari, K., Mursula, K., Usoskin, I. G., & Kovaltsov, G. A. 2006, Solar Phys., 238, 391

Athay, R. G. 1986, Astrophys. J., 308, 975

Berggren, A.-M., Beer, J., Possnert, G., Aldahan, A., Kubik, P., Christl, M., Johnsen, S. J., Abreu, J., & Vinther, B. M. 2009, Geophys. Res. Lett., 36, 11801

Billings, D. E. 1966, A Guide to the Solar Corona (New York: Academic Press)

Eddy, J. A. 1976, Science, 192, 1189

Fisher, G. H., Longcope, D. W., Metcalf, T. R., & Pevtsov, A. A. 1998, Astrophys. J., 508, 885

Grant, R. 1852, History of physical astronomy from the earliest ages to the middle of the nineteenth century ..., Harvard astronomy preservation microfilm project (Bohn)

Hoyt, D. V., & Schatten, K. H. 1996, Solar. Phys., 165, 181

Koutchmy, S., & Lamy, P. L. 1985, in Astrophysics and Space Science Library, Vol. 119, IAU Colloq. 85: Properties and Interactions of Interplanetary Dust, ed. R. H. Giese & P. Lamy, 63–74

Linker, J. A., Mikic, Z., Riley, P., Downs, C., Lionello, R., Henney, C., & Arge, C. N. 2012, Proceedings of Solar Wind 13, AIP Conf. Proc., 1539, 26

Lionello, R., Linker, J. A., & Mikić, Z. 2009, Astrophys. J., 690, 902

Lockwood, M., & Owens, M. J. 2011, J. Geophys. Res., 116, 4109

Luterbacher, J. 2001, History and climate: memories of the future, 29

Mackay, D. H. 2003, Sol Phys., 213, 173

Manley, G. 2011, Weather, 66, 133

Maunder, E. W. 1894, Knowledge, 17, 173

McCracken, K., Beer, J., Steinhilber, F., & Abreu, J. 2011, Space Sci. Rev.

McCracken, K. G., & Beer, J. 2007, Journal of Geophysical Research (Space Physics), 112, 10101

McCracken, K. G., Beer, J., & McDonald, F. B. 2005, ISSI Scientific Reports Series, 3, 83

McCracken, K. G., McDonald, F. B., Beer, J., Raisbeck, G., & Yiou, F. 2004, Journal of Geophysical Research (Space Physics), 109, 12103

Mikić, Z., Linker, J. A., Lionello, R., Riley, P., & Titov, V. 2007, in Astronomical Society of the Pacific Conference Series, Vol. 370, Solar and Stellar Physics Through Eclipses, ed. O. Demircan, S. O. Selam, & B. Albayrak, 299–+

Parker, E. N. 1976, in IAU Symposium, Vol. 71, Basic Mechanisms of Solar Activity, ed. V. Bumba & J. Kleczek, 3

Pevtsov, A. A., Fisher, G. H., Acton, L. W., Longcope, D. W., Johns-Krull, C. M., Kankelborg, C. C., & Metcalf, T. R. 2003, Astrophys. J., 598, 1387

Reimer, P. J., Baillie, M. G. L., Bard, E., Bayliss, A., Beck, J. W., Bertrand, C. J. H., Blackwell, P. G., Buck, C. E., Burr, G. S., Cutler, K. B., Damon, P. E., Edwards, R. L., Fairbanks, R. G., Friedrich, M., Guilderson, T. P., Hogg, A. G., Hughen, K. A., Kromer, B., McCormac, G., Manning, S., Ramsey, C. B., Reimer, R. W.,

Remmele, S., Southon, J. R., Stuiver, M., Talamo, S., Taylor, F. W., van der Plicht, J., & Weyhenmeyer, C. E. 2004, Radiocarbon, 46, 1029

Réthly, A., & Berkes, Z. 1963, Nordlichtbeobachtungen in Ungarn, 1523-1960 (Verlag der Ungarischen Akademie der Wissenschaften)

Riley, P. 2010, in Twelfth International Solar Wind Conference, Am. Inst. Phys. Conf. Proc., ed. M. Maksimovic, K. Issautier, N. Meyer-Vernet, M. Moncuquet, & F. Pantellini, Vol. 1216, 323

Riley, P., Linker, J. A., Lionello, R., & Mikic, Z. 2012a, J. Atmos. Solar-Terr. Phys., 83, 1

Riley, P., Linker, J. A., & Mikić, Z. 2001, J. Geophys. Res., 106, 15889

Riley, P., Lionello, R., Linker, J. A., Mikic, Z., Luhmann, J., & Wijaya, J. 2011, Solar Phys., 145

—. 2012b, Solar Phys., 274

Riley, P., Lionello, R., Mikić, Z., Linker, J., Clark, E., Lin, J., & Ko, Y.-K. 2007, Astrophys. J., 655, 591

Riley, P., & Luhmann, J. G. 2012, Solar Phys., 277, 355

Riley, P., Mikic, Z., Linker, J. A., McComas, D. J., & Schwadron, N. A. 2009, AGU Fall Meeting Abstracts, A1496+

Schrijver, C. J., Livingston, W. C., Woods, T. N., & Mewaldt, R. A. 2011, Geophys. Res. Lett., 38, 6701

Schröder, W. 1992, J. Geomagn. Geoelectr, 44, 119

Schwadron, N. A., Connick, D. E., & Smith, C. 2010, Ap. J. Lett., 722, L132

Siscoe, G. L. 1980, Reviews of Geophysics and Space Physics, 18, 647

Smith, E. J., & Balogh, A. 2008, Geophys. Res. Lett., 35, 22103

Smith, E. J., & Marsden, R. G. 2003, Geophys. Res. Lett., 30, 1

Solanki, S. K., Usoskin, I. G., Kromer, B., Schüssler, M., & Beer, J. 2004, Nature, 431, 1084

Soon, W., & Yaskell, S. 2003, Maunder Minimum: And the Variable Sun-Earth Connection (World Scientific Publishing Company Incorporated)

Sporer, E. 1887, Vierteljahrsschr. Astron. Ges. Leipzig, 22, 323

Steinhilber, F., Abreu, J. A., Beer, J., Brunner, I., Christl, M., Fischer, H., Heikkilä, U., Kubik, P. W., Mann, M., McCracken, K. G., et al. 2012, Proceedings of the National Academy of Sciences, 109, 5967

Stevens, M., Linker, J. A., & Riley, P. 2012, J. Atmos. Solar-Terr. Phys., in press

Suess, S. T. 1979, Plan. Space Sci., 27, 1001

Svalgaard, L. 2010, ArXiv e-prints

Svalgaard, L. 2011, Proceedings of the International Astronomical Union, 7, 27

Svalgaard, L., & Cliver, E. W. 2007, Astrophys. J. Lett., 661, 203

Usoskin, I. G. 2008, Living Reviews in Solar Physics, 5, 3

Usoskin, I. G., Bazilevskaya, G. A., & Kovaltsov, G. A. 2011, Journal of Geophysical Research (Space Physics), 116, 2104

Usoskin, I. G., Solanki, S. K., Schüssler, M., Mursula, K., & Alanko, K. 2003, Physical Review Letters, 91, 211101

Wang, Y.-M., & Sheeley, N. R. 1995, Astrophys. J. Lett., 447, L143

Wang, Y.-M., & Sheeley, Jr., N. R. 2013, Ap. J., 764, 90

Wing, V. 1656, Astronomica Instaurata, Or, A New and Compendious Restauration of Astronomie: In Four Parts ... Whereunto is Added, a Short Catalogue of All the Most Accurate and Remarkable Coelestiall Observations, that Have Been Made by Tycho, Longomontanus, Gassendus, the Landgrave of Hassia, and Others (R. and W. Leybourn)

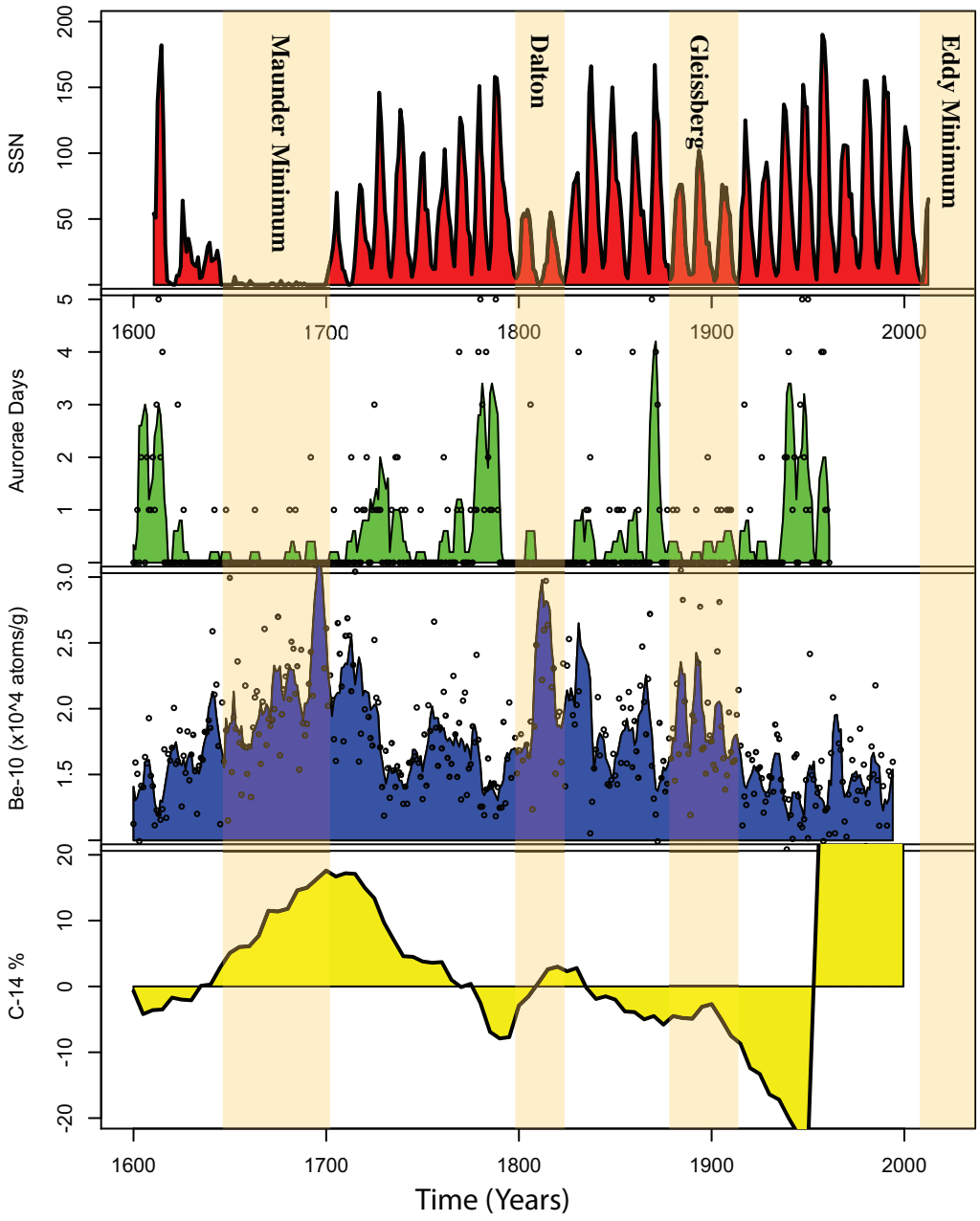

Fig. 1.— The evolution of various solar-related parameters from 1600 through 2012. (a) the yearly sunspot number (Svalgaard 2010). (b) the number of aurora per year (Réthly & Berkes 1963). (c) Beryllium-10 measurements (Berggren et al. 2009). (d) Carbon-14 measurements (Reimer et al. 2004) . The circles in (b) and (c) represent the original data at yearly resolution. See text for more details.

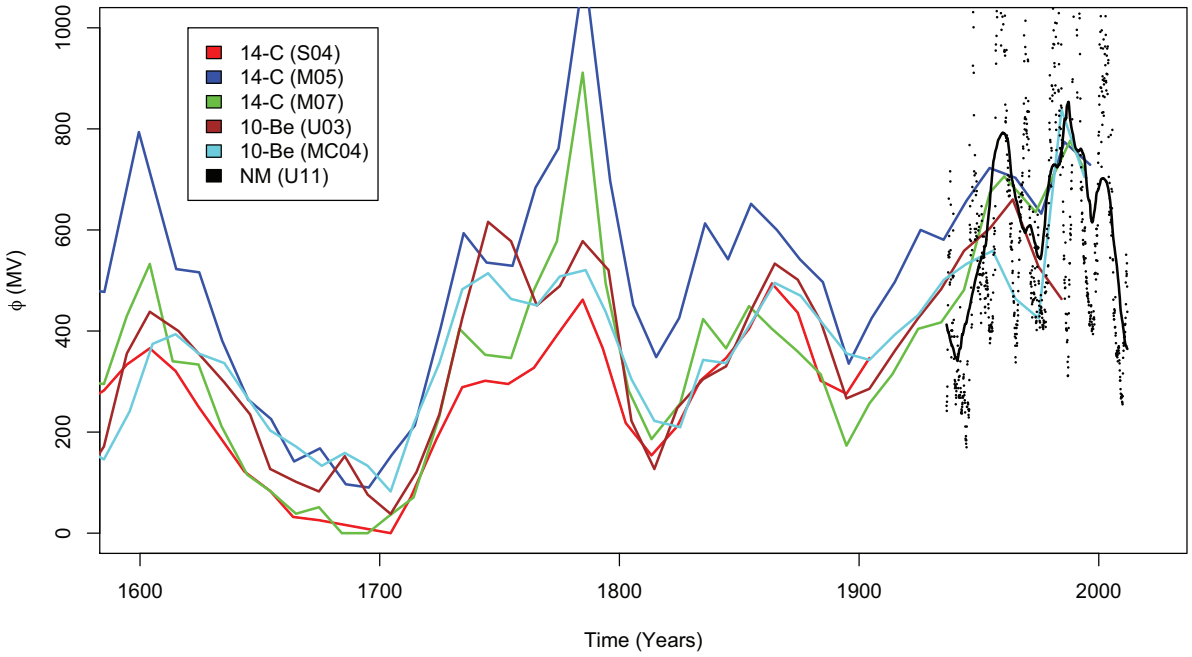

Fig. 2.— Temporal evolution of a selection of estimates for the modulation potential (ϕ). Following Usoskin (2008), S04 refers to Solanki et al. (2004), M05 refers to McCracken et al. (2005), M07 refers to McCracken & Beer (2007), U03 refers to Usoskin et al. (2003), MC04 refers to McCracken et al. (2004), and U11 refers to Usoskin et al. (2011). The first three profiles are based on Carbon-14 records, the next two are based on Beryllium-10, and the final profile shows direct neutron monitor measurements both on monthly averages (dots) and an 11-year running mean (solid black curve).

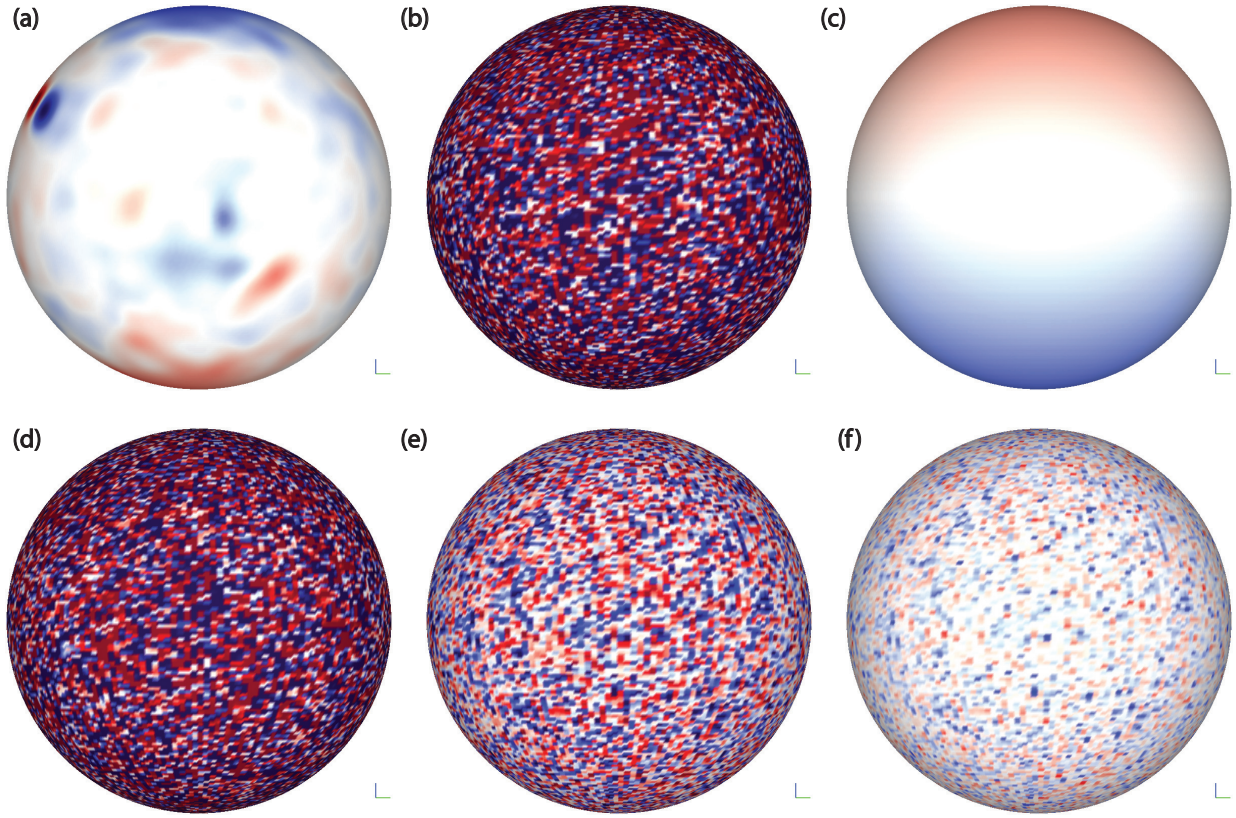

Fig. 3.— Comparison of possible configurations of the Sun's photospheric magnetic field during the Maunder Minimum period: (a) CR 2085; (b) parasitic polarity (±3.3G) plus large-scale dipole (3.3G); (c) Large-scale dipole only (3.3G); (d) parasitic polarity (±3.3G) plus large-scale dipole (1G); (e) parasitic polarity only (±10G); and (f) parasitic polarity (±3.3G).

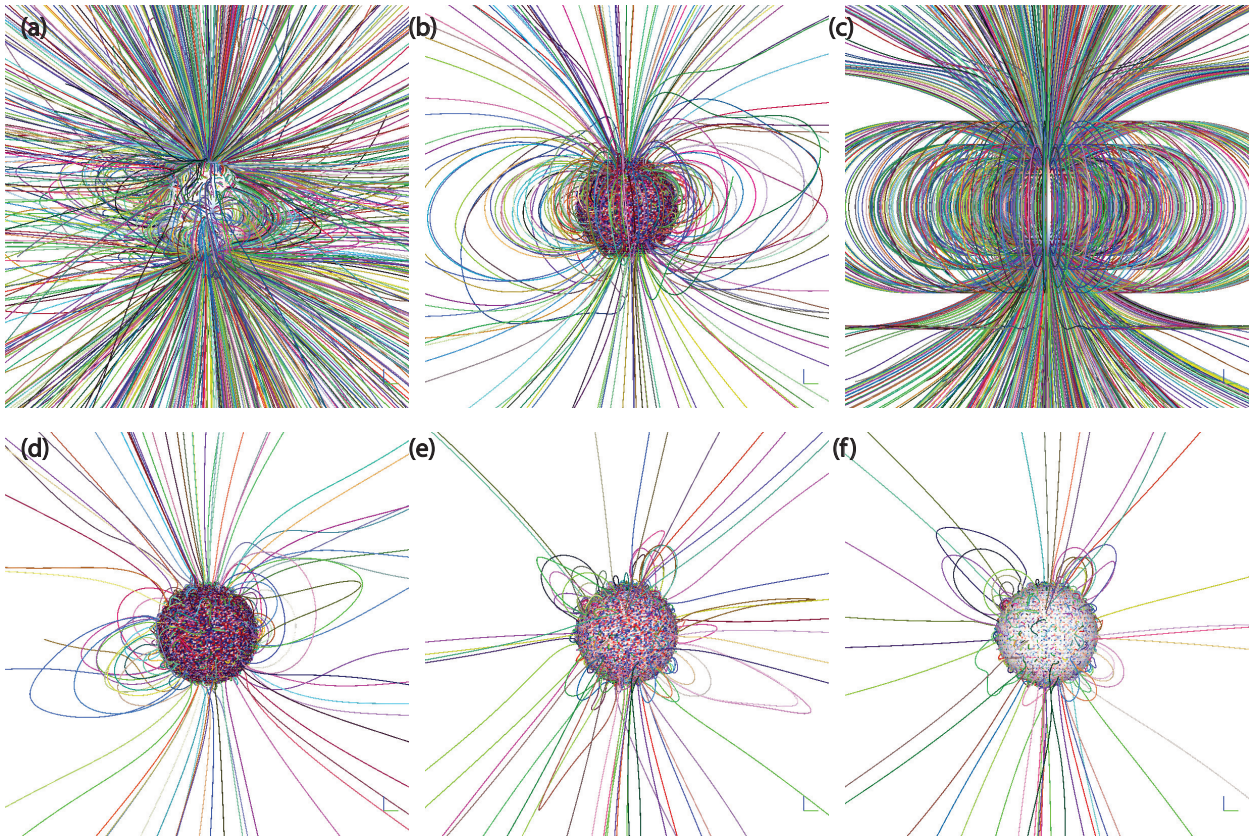

Fig. 4.— As Figure 3 but showing a selection of magnetic field lines drawn from a grid separated by 10° in latitude and longitude.

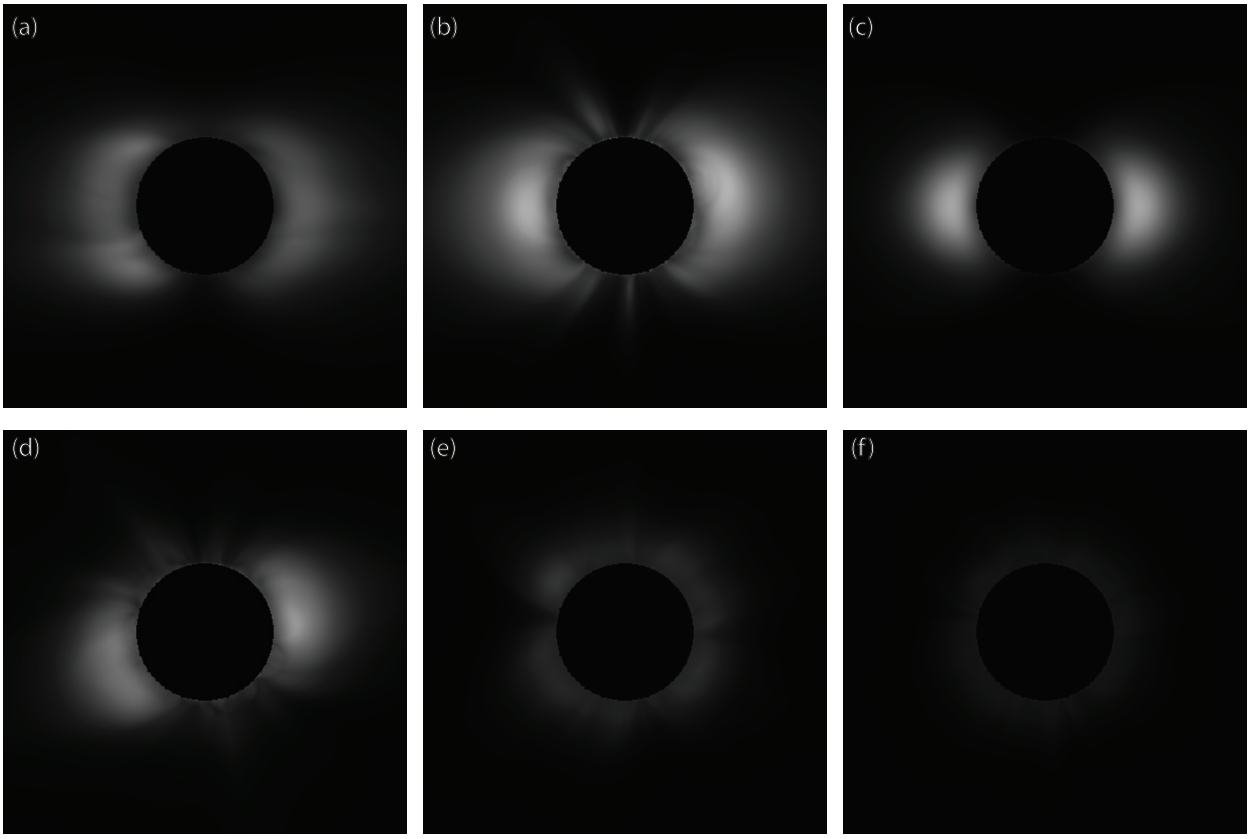

Fig. 5.— As Figure 3 but showing simulated polarized brightness.

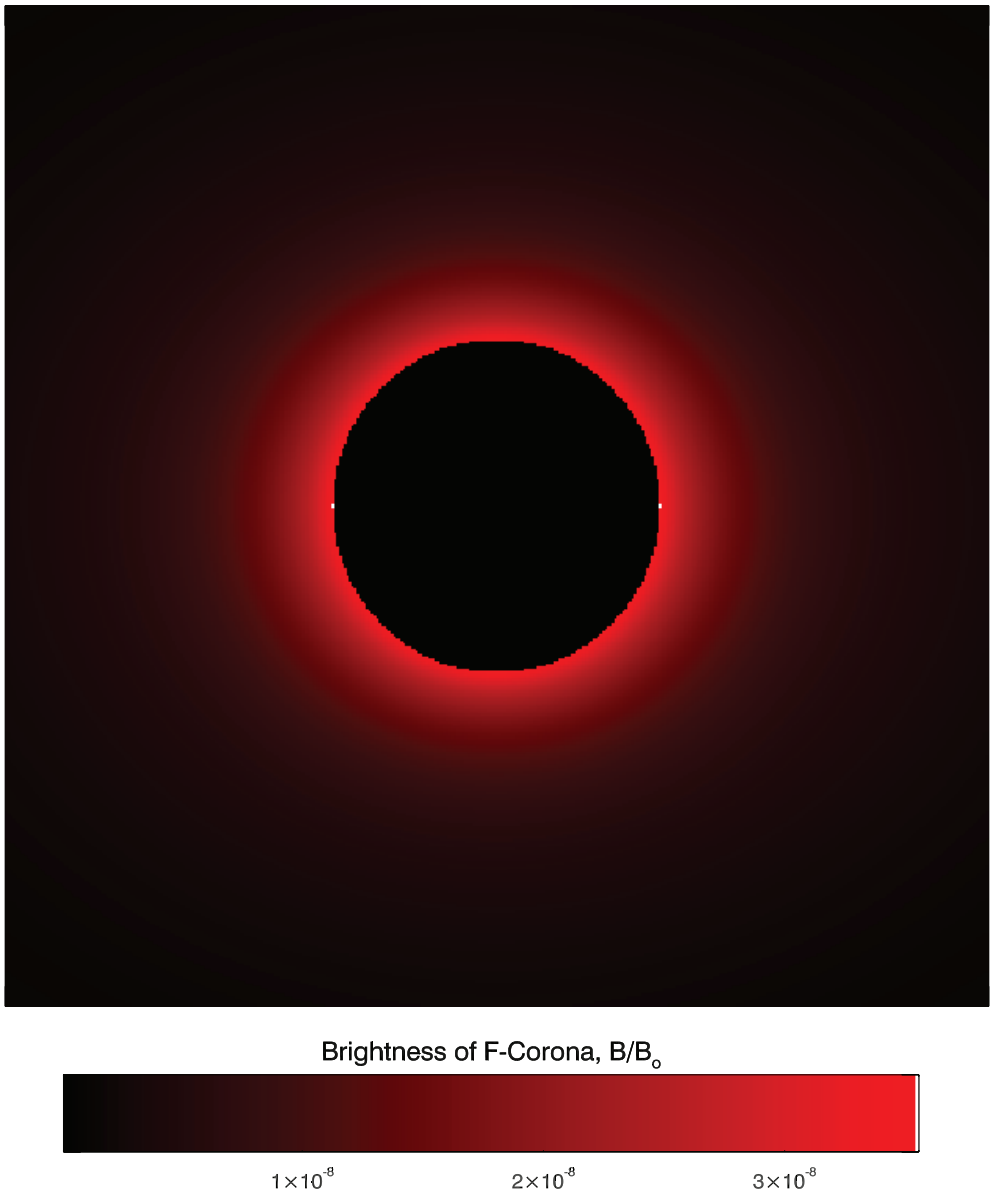

Fig. 6.— Simulated image of the F corona, based on the formula by Koutchmy & Lamy (1985).

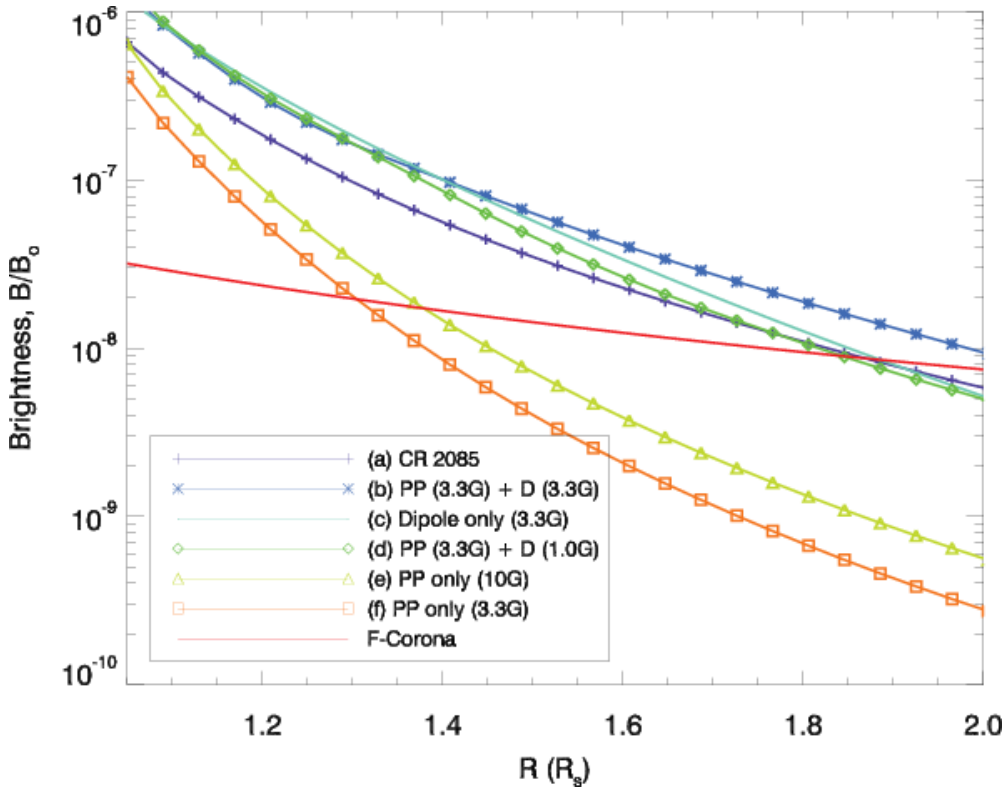

Fig. 7.— Comparison of radial fall-off in brightness for the six model results shown in Figure 5 with the brightness profile computed for the F-corona (red).

Table 1: Open flux estimates.

Model	Description	Open Flux
(a)	CR 2085 (06/26/09-07/23/09)	1.0 nT
(b)	Parasitic polarity (±3.3 G) + Large-scale dipole (3.3G)	2.4 nT
(c)	Large-scale dipole only (3.3G)	2.2 nT
(d)	Parasitic polarity + Large-scale dipole (1G)	1.2 nT
(e)	Parasitic polarity only (±10 G)	0.29 nT
(f)	Parasitic polarity only (±3.3 G)	0.08 nT

Table 2: Summary of observational evidence for each of two possible Maunder Minimum scenarios.

Observation	2008 Sun	Ephemeral Sun	Notes
SSN	×	✓	Strictly speaking, 2008/2009 cannot represent ∼ 1700 because sunspots have not been absent for the last 70 years.
Aurora	?	✓	Difficult to assess because historical records are not currently maintained, and current measures are limited to space era.
^{10}Be	×	✓	When coupled with neutron monitor measurements and converted to modulation potential, 2008 was significantly different than 1700.
^{14}C	×	✓	Unfortunately, natural ^{14}C measurements cannot be extended beyond 1950.
Coronal Structure	×	✓	Eclipse observations during MM are not unambiguous. However, argument can be made that a 2008 eclipse would have been noted.
Red Glow	×	✓	Reports of an "erie" red glow are suggestive of an F-corona (and commensurately fainter, or absent K-corona).
22-year Periodicity	✓	×	Continued solar cycle suggests that circulation still proceeding, implying that polar fields continued to build-up and decay.